Molecular Biology of the Cell
Vol. 17, 3819–3831, September 2006

Inhibition of Transforming Growth Factor-β1–induced Signaling and Epithelial-to-Mesenchymal Transition by the Smad-binding Peptide Aptamer Trx-SARA

Bryan M. Zhao* and F. Michael Hoffmann*†

*McArdle Laboratory for Cancer Research and †Laboratory of Genetics, University of Wisconsin-Madison, Madison, WI 53706

Submitted October 31, 2005; Revised May 10, 2006; Accepted June 7, 2006
Monitoring Editor: Carl-Henrik Heldin

Overexpression of the inhibitory Smad, Smad7, is used frequently to implicate the Smad pathway in cellular responses to transforming growth factor β (TGF-β) signaling; however, Smad7 regulates several other proteins, including Cdc42, p38MAPK, and β-catenin. We report an alternative approach for more specifically disrupting Smad-dependent signaling using a peptide aptamer, Trx-SARA, which comprises a rigid scaffold, the *Escherichia coli* thioredoxin A protein (Trx), displaying a constrained 56-amino acid Smad-binding motif from the Smad anchor for receptor activation (SARA) protein. Trx-SARA bound specifically to Smad2 and Smad3 and inhibited both TGF-β–induced reporter gene expression and epithelial-to-mesenchymal transition in NMuMG murine mammary epithelial cells. In contrast to Smad7, Trx-SARA had no effect on the Smad2 or 3 phosphorylation levels induced by TGF-β1. Trx-SARA was primarily localized to the nucleus and perturbed the normal cytoplasmic localization of Smad2 and 3 to a nuclear localization in the absence of TGF-β1, consistent with reduced Smad nuclear export. The key mode of action of Trx-SARA was to reduce the level of Smad2 and Smad3 in complex with Smad4 after TGF-β1 stimulation, a mechanism of action consistent with the preferential binding of SARA to monomeric Smad protein and Trx-SARA-mediated disruption of active Smad complexes.

INTRODUCTION

Transforming growth factor-β (TGF-β) is a pluripotent cytokine that regulates diverse biological processes such as cell proliferation, differentiation, apoptosis, and epithelial-to-mesenchymal transition (EMT; ten Dijke *et al.*, 2002; Siegel and Massague, 2003). TGF-β signaling has also been associated with fibrosis and cancer (Derynck *et al.*, 2001; Leask and Abraham, 2004; Flanders, 2004). TGF-β signaling initiates when the TGF-β ligand binds to and actives the type II and type I receptor kinases, resulting in Smad2 and Smad3 phosphorylation. Phosphorylated Smad2 and Smad3 form heterodimeric and heterotrimeric complexes with Smad4 that accumulate in the nucleus and bind over two dozen different transcription factors, coactivators, and corepressors to activate or inhibit the expression of specific target genes (Derynck and Zhang, 2003; Shi and Massague, 2003; ten Dijke and Hill, 2004; Feng and Derynck, 2005; Massague *et al.*, 2005). TGF-β also activates several Smad-independent signaling pathways that involve proteins such as Tak1, ERK/MAPK, and RhoA (Derynck and Zhang, 2003).

Inhibition of TGF-β signaling is an important tool for elucidating the multiple biological functions of TGF-β and has become of significant interest as a potential therapeutic strategy in fibrotic diseases and metastatic cancer (Dumont and Arteaga, 2003; Yingling *et al.*, 2004). The ligand itself has been the target for several methods of inhibition include blocking synthesis of the ligand with antisense (Fakhrai *et al.*, 1996), binding peptide inhibitors to the ligand (Santiago *et al.*, 2005), or sequestering the ligand using neutralizing antibodies (Ziyadeh *et al.*, 2000; Mead *et al.*, 2003) or soluble TGF-β–binding proteins (Komesli *et al.*, 1998; Kolb *et al.*, 2001; Bandyopadhyay *et al.*, 2002). The TGF-β receptors have also been targeted to disrupt the pathway by using neutralizing antibodies to the receptor (Kasuga *et al.*, 2001), dominant-negative forms of the receptors (Gorelik and Flavell, 2001), dominant-negative forms of Smad2 or Smad3 that bind to receptor but cannot be phosphorylated (Macias-Silva *et al.*, 1996) or by inhibiting the kinase activity of the receptor with small molecule compounds (Laping *et al.*, 2002; DaCosta Byfield *et al.*, 2004; Singh *et al.*, 2004; Grygielko *et al.*, 2005). Chemical inhibitors of the kinase activity, such as SB431542, block the phosphorylation of Smad2 and Smad3 (Inman *et al.*, 2002a) and inhibit TGF-β–induced cell proliferation and motility of glioma cells (Hjelmeland *et al.*, 2004) or fibrosis in skin fibroblasts (Mori *et al.*, 2004). Small molecule inhibitors have also been used to inhibit Smad-independent TGF-β activation of, for example, c-Abl (with imatinib mesylate; Daniels *et al.*, 2004), phosphatidylinositol 3-OH kinase (with LY294002; Bakin *et al.*, 2000), p38 mitogen–activated protein kinase (with SB202190; Bakin *et al.*, 2002), or mitogen activated protein kinase (with U0126; Xie *et al.*, 2004).

A natural inhibitor of TGF-β signaling, the inhibitory Smad, Smad7, is frequently constitutively expressed, or overexpressed, to demonstrate that Smad-dependent signaling is involved in a specific gene expression or biological response to TGF-β. Smad7 is induced by TGF-β and binds to both TGF-β type I receptor and bone morphogenetic protein (BMP) type I receptors to inhibit phosphorylation of the regulated Smads (R-Smads; Nakao *et al.*, 1997; Souchelnytskyi *et al.*, 1998; Mochizuki *et al.*, 2004) and to target the

This article was published online ahead of print in *MBC in Press* (http://www.molbiolcell.org/cgi/doi/10.1091/mbc.E05–10–0990) on June 14, 2006.

Address correspondence to: F. Michael Hoffmann (fmhoffma@wisc.edu).

type I receptors for proteolytic degradation (Kavsak *et al.*, 2000; Ebisawa *et al.*, 2001). Smad7 targets the type I receptors for degradation in the lipid raft-caveolar internalization pathway by recruiting Smurf ubiquitin ligase to the receptors (Kavsak *et al.*, 2000; Di Guglielmo *et al.*, 2003; Murakami *et al.*, 2003). Smad7 also functions as a scaffold or adaptor protein to assemble GADD34 and protein phosphatase 1 (PP1) at the activated type I receptor, where PP1 de-phosphorylates and inactivates the type 1 receptor (Shi *et al.*, 2004). However, Smad7 appears to have a variety of other functions. In some cells, e.g., PC-3U and HaCaTs, Smad7 mediates TGF-β–induced apoptosis (Landstrom *et al.*, 2000). Overexpression of Smad7 interferes with the prosurvival functions of NFκB and activates apoptosis through stress-activated MAPKs (Lallemand *et al.*, 2001; Yu *et al.*, 2002; Undevia *et al.*, 2004). Smad7 serves as a scaffold for assembling a complex of TAK1-MKK3 and p38 MAPK that causes activation of p38MAPK in PC3U cells (Edlund *et al.*, 2003). One function of activated p38 MAPK in these cells is to inactivate GSK-3β, leading to stabilization and activation of β-catenin–mediated apoptosis (Edlund *et al.*, 2005). Smad7 also forms a protein complex with β-catenin and LEF1/TCF in response to TGF-β to facilitate transcriptional activation of β-catenin responsive genes such as Myc (Edlund *et al.*, 2005). This may be cell type specific in that Smad7 activates a different MAPK pathway, the SAPK/JNK pathway, in MvLu1 cells and MDCK cells to trigger apoptosis (Lallemand *et al.*, 2001). Smad7 is localized in the nucleus and can also interact with histone deacetylase 1 (Bai and Cao, 2002). Smad7 is also reported to mediate TGF-β activation of Cdc42, reorganization of actin filaments, and membrane ruffling (Edlund *et al.*, 2004). This multitude of Smad7 functions indicates that the consequences of overexpressing Smad7 perhaps should not be interpreted as simple inhibition of Smad-dependent signal transduction.

We have been interested in targeting the transcriptionally active Smad complexes to inhibit signaling and provide selective inhibition of Smad-dependent TGF-β responses. To develop such reagents, we are identifying constrained peptide inhibitors that are targeted to Smad proteins (Cui *et al.*, 2005). Constrained peptide motifs expressed on a rigid scaffold protein, also called peptide aptamers, have been used to disrupt signal transduction events in mammalian cells by binding to a target protein and disrupting normal protein–protein interactions, e.g., cyclin-dependent kinase 2 (Colas *et al.*, 1996), E2F-DP1 (Fabbrizio *et al.*, 1999), p53-mdm2 (Bottger *et al.*, 1997), epidermal growth factor (EGF) receptor-Stat3 interaction (Buerger *et al.*, 2003), and Stat3-DNA binding or Stat3 dimerization (Nagel-Wolfrum *et al.*, 2004). The development of protein scaffolds began with the recognition that immunoglobulins function through the use of a conserved framework region and a spatially defined hypervariable region. Subsequently several proteins of small size, high stability and ease of production, such as *E. coli* thioredoxin A (Trx), have been tested as protein scaffolds (Skerra, 2000). The benefits of expressing a constrained peptide on a scaffold can include improved binding affinity, e.g., a peptide aptamer that inhibits cyclin-dependent kinase 2 has an IC_{50} 1000-fold lower than the free 20-amino acid peptide (Colas *et al.*, 1996). The aptamers to cdk2 also showed selective inhibition in blocking the interaction of cdk2 with histone H1 but not affecting the interaction with Rb (Cohen *et al.*, 1998). Importantly, peptide aptamers on the *E. coli* thioredoxin A scaffold are efficiently expressed in mammalian cells, e.g., expression of a Trx peptide aptamer from a CMV promoter in Saos-2 cells inhibited cell cycle progression (Cohen *et al.*, 1998), and introduction of a 12 amino acid Mdm2-binding Trx peptide aptamer into cells caused an accumulation of p53 protein and activation of p53-responsive reporter genes (Bottger *et al.*, 1997). We have reported that Trx aptamers containing peptides from xFoxH1b and Lef1 bind to Smads and selectively inhibit TGF-β responsive reporter genes (Cui *et al.*, 2005). The Trx-Lef1 aptamer inhibited TGF-β activation of the TwnTop-luciferase reporter and Trx-XFoxH1b aptamer inhibited TGF-β activation of the A3-luciferase reporter. The activities of several other reporter genes were not altered by either aptamer (Cui *et al.*, 2005).

We have now generated a peptide aptamer that displays the Smad-binding domain from the protein "Smad anchor for receptor activation" (SARA) on the Trx scaffold. SARA was originally identified as a Smad2-binding protein and is localized to the early endosomal membrane through a double zinc finger FYVE domain (Tsukazaki *et al.*, 1998; Itoh *et al.*, 2002). SARA also binds to the type I TGF-β receptor and recruits Smad2 or Smad3 to the type I receptor for phosphorylation (Tsukazaki *et al.*, 1998). Phosphorylation of Smad by the type I receptor leads to release of the Smad from SARA and assembly of multimeric Smad2/4 and Smad3/4 complexes (Tsukazaki *et al.*, 1998; Qin *et al.*, 2002). The Smad-binding domain (SBD) of SARA, amino acids 665–750, is sufficient to bind Smad2 or Smad3 in vitro and was cocrystallized with the MH2 domain of Smad2 (Wu *et al.*, 2000; Qin *et al.*, 2002). Three structural motifs of the SARA SBD bind along the hydrophobic groove of the Smad MH2 domain. The MH2 monomer bound to SARA is in a different conformation than the MH2 incorporated into a heterotrimeric complex with Smad4, consistent with biochemical data showing that SARA preferentially binds to the monomeric form of Smad and can disrupt the Smad3–4 complex in vitro (Wu *et al.*, 2000).

MATERIALS AND METHODS

Cell Lines and Cell Culture Conditions

Mouse mammary gland (NMuMG) cells were obtained from Dr. Caroline Alexander (University of Wisconsin-Madison, WI). NMuMG cells were maintained in DMEM and supplemented with 10% fetal bovine serum (FBS), 10 μg/ml insulin, 100 μg/ml penicillin, and 100U/ml streptomycin. 293 cells were obtained from ATCC (Manassas, VA) and grown in 10% DMEM and supplemented with 10% FBS, 100 μg/ml penicillin, and 100 U/ml streptomycin. All cells were grown at 37°C in 5% CO_2. TGF-β1 was purchased from R&D Systems (Minneapolis, MN). TNF-α was purchased from Sigma-Aldrich (St. Louis, MO). Human recombinant EGF was purchased from Upstate Signalling (Charlottesville, VA).

Generation of Peptide Aptamers

For mammalian expression of the aptamers, fragments of human SARA (accession AF104304) were obtained by PCR using primers with terminal RsrII sites and cloned into the unique RsrII site of pCI-NLS-HA-Trx (Cui *et al.*, 2005). The specific amino acid sequences included in each aptamer are shown in Figure 1.

Production of Retrovirus and Generation of Infected Cells and Flow Cytometry

The hemagglutinin (HA)-tagged Trx-SARA and the Flag-tagged Smad7 were cloned into the pCMMV-IRES-GFP vector (Ory *et al.*, 1996; Kennedy and Sugden, 2003) using the NotI restriction site. Plasmids were transfected in 293 cells to generate virus as described previously (Cui *et al.*, 2005). NMuMG cells were infected with virus multiple times to generate $NMuMG^{Trx\text{-}GA}$, $NMuMG^{Trx\text{-}SARA}$, and $NMuMG^{Smad7}$cells. Cells were sorted by flow cytometry (UWCCC Flow Cytometry Facility, Madison, WI) for GFP intensity, and the brightest 10% of the cells were collected in 2 ml of FBS. These cell populations were expanded and used for all experiments.

Immunoblotting and Coimmunoprecipitation

Cells were washed with ice-cold phosphate-buffered saline (PBS) and lysed with TNE buffer (10 mM Tris-HCl, pH 8.0, 100 mM NaCl, 1% Nonidet P-40, 1 mM EDTA) supplemented with proteinase inhibitors (Roche Applied Science, Indianapolis, IN) and phosphatase inhibitors (1 mM EDTA, 20 mM NaF,

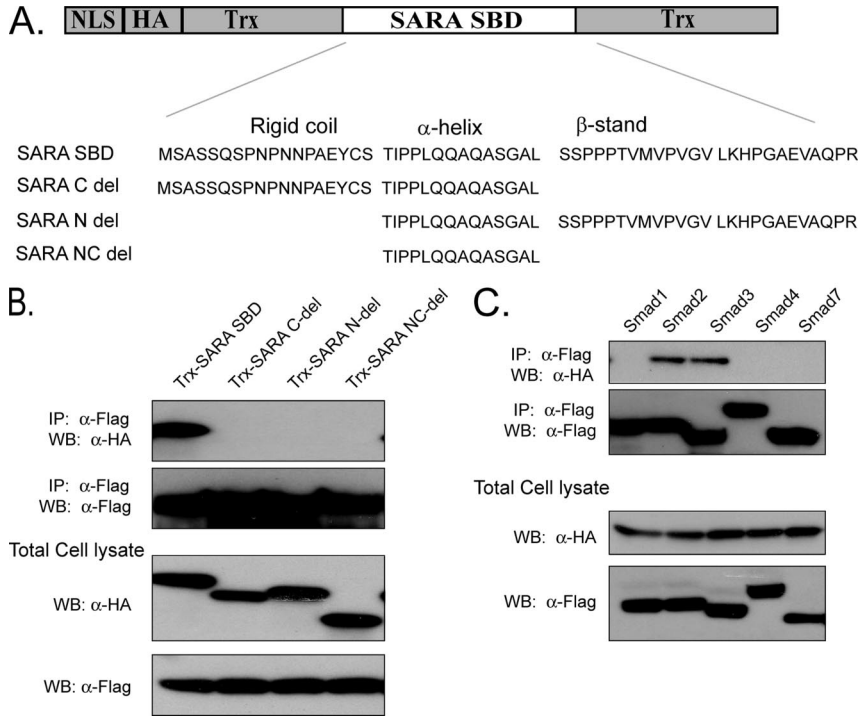

Figure 1. Trx-SARA specifically interacts with Smad2 and Smad3. (A) Four different portions of SARA SBD were cloned into Trx to determine whether all three secondary structural motifs, the rigid coil, the alpha helix, and the beta strand were required for the Trx-SARA aptamer to bind to Smad. HA and NLS denote the HA-epitope tag and the nuclear localization sequence fused to the N-terminus of Trx for detection of expression and localization in mammalian cells. (B) HA-tagged Trx-SARA aptamer expression plasmids were cotransfected into 293 cells with the Flag-Smad2 expression plasmid. Total cell lysates were prepared, immunoprecipitated with anti-Flag antibody, resolved by SDS-PAGE, and analyzed for HA-tagged Trx-SARA aptamers by immunoblotting with anti-HA antibody. Only the full-length SBD in Trx associated with Smad2. Total cell lysates (lower two panels) were probed with anti-HA or anti-Flag antibodies to confirm similar expression levels in all four transfections. (C) The HA-Trx-SARA expression plasmid was cotransfected into 293 cells with expression plasmids for Flag-tagged Smads (Smad1, Smad2, Smad3, Smad4, or Smad7). Total cell lysates were prepared, immunoprecipitated with anti-Flag antibody, resolved by SDS-PAGE, and analyzed for HA-tagged Trx-SARA aptamers by immunoblotting with anti-HA antibody. Total cell lysates (lower two panels) were probed with anti-HA or anti-Flag antibodies to confirm similar expression levels in all five transfections.

and 1 mM sodium orthovanadate). Total cell lysates were centrifuged at 14,000 rpm for 10 min at 4°C. Protein concentrations were determined by BCA assay kit (Pierce, Rockford, IL). Protein A/G plus agarose beads (Santa Cruz Biotechnology, Santa Cruz, CA) were used in coimmunoprecipitation assays. Total cell lysates or immunoprecipitates were resolved by 4–20% SDS-PAGE and transferred to PVDF membrane. The following antibodies were used: rabbit phospho-Smad2(Ser465/467), rabbit p38, phospho-p38, rabbit p42/44, phospho-p42/44, Akt and phospho-Akt (Cell Signalling Technology, Beverly, MA), rabbit anti-phospho-Smad3 (gift from Ed Leof, Mayo Clinic. Rochester, MN), *N*-cadherin, SP1, and Smad4 (B-8; Santa Cruz Biotechnology), anti-E-cadherin (BD Biosciences, San Jose, CA), β-actin, vimentin, Flag-M2, and β-tubulin (Sigma-Aldrich), Smad2 and Smad3 (Zymed Laboratories, South San Francisco, CA), and HA-peroxidase (Roche Applied Science, Indianapolis, IN).

Reporter Gene Assays

About 10,000 NMuMG cells were seeded in 12-well plates. After 24 h, NMuMG cells were transfected with reporter constructs and CMV-β-galactosidase plasmid using LipofectAMINE 2000 (Invitrogen, Carlsbad, CA) or Fugene 6 (Roche Applied Science). Six hours after the transfection, cells were treated with or without TGF-β (100 pM) in 0.2% FBS DMEM. After 20 h, cells were lysed and luciferase (Promega, Madison, WI) and β-galactosidase assays (Galacto-Star, Tropix, Bedford, MA) were performed according to manufacturer's instructions. For the 3xκb-luc reporter assay, NMuMG cells were treated with 10 ng/ml TNF-α for 12 h. Luciferase values were normalized to the β-gal activity.

Immunocytochemistry

Cells were grown on coverslips (VWR) or eight-well chamber slides (VWR). After the TGF-β (100pM) treatment, cells were fixed with 4% (wt/vol) paraformaldehyde in PBS and permeabilized with 0.5% Triton X-100 in PBS for 1 min. Cells were incubated with blocking solution (3% BSA in PBS). Primary antibodies were added at 1:200 dilutions in blocking solution, incubated for at least 1 h at room temperature, and then washed three times with 0.05% Triton X-100 in PBS. Subsequently, secondary antibodies diluted in blocking solution were added and incubated for 30 min. Finally, cells were washed with PBS and mounted with DAPI (Santa Cruz Biotechnology) and visualized by fluorescence microscopy (Carl Zeiss, Thornwood, NY). The following antibodies were used: Texas red–conjugated phalloidin (Sigma-Aldrich), anti-Smad2 and anti-Smad3 antibody (Zymed Laboratories), and anti-E-cadherin antibody (BD Biosciences). Alexa Fluor 594 goat anti-rabbit IgG, Alexa Fluor 594 anti-mouse, and Alexa Fluor 594 anti-HA mouse antibody (16B12) were purchased from Invitrogen. Images were processed using Adobe Photoshop software (Adobe Systems, Mountain View, CA).

Cell Fractionation

Cells grown to 80% confluency were washed with ice-cold PBS. Cytoplasmic and nuclear fractions were extracted using Nuclear and Cytoplasmic Extraction Reagent (Pierce, Rockford, IL) following the manufacturer's instructions. Nuclear and cytoplasmic protein concentrations were determined by BCA assay (Pierce).

Biotinylated SBE4 Oligonucleotide Pulldown Assay

Cells grown in P100 plates were lysed with TNE buffer (described above). Equal amounts of total cell lysate were incubated overnight at 4°C with streptavidin-agarose beads (Pierce) and 1 μg of the double-stranded SBE4 oligonucleotide (biotin-5′-GTACCCAGACAGTCAGACAGTCAGACAGTCAGACAGTC-3′; Warner *et al.*, 2003). Streptavidin-agarose beads were washed four times with TNE buffer. Bound proteins were resolved by SDS-PAGE on a 4–20% gel.

RESULTS

Trx-SARA Aptamer Binds Smad2

In a previous study, the minimum Smad-binding domain (SBD) of SARA was identified as amino acids 665–721 (Wu *et al.*, 2000). We introduced this 56 amino acid SARA SBD into the active site loop of *E. coli* Trx to generate the Trx-SARA aptamer. An HA epitope tag and nuclear localization sequence were added to the N-terminus of the Trx scaffold (Figure 1A). The SARA SBD contains three motifs: the rigid coil, the amphipathic α-helix and the β-strand, which are all implicated in binding to the hydrophobic groove of the Smad MH2 domain (Wu *et al.*, 2000; Figure 1A). To determine the importance of these secondary structure elements in mediating the aptamer–Smad interaction, we constructed a series of deletion mutants of the Trx-SARA, the N-terminal deletion (removes rigid coil), the C-terminal deletion (removes the β-strand) and the N and C terminal deletion (removes both the rigid coil and the β-strand; Figure 1A). We tested whether the Trx-SARA SBD aptamer bound to Smad2 in mammalian cells by coimmunoprecipitation. Expression plasmids for Flag-tagged Smad2 and HA-tagged

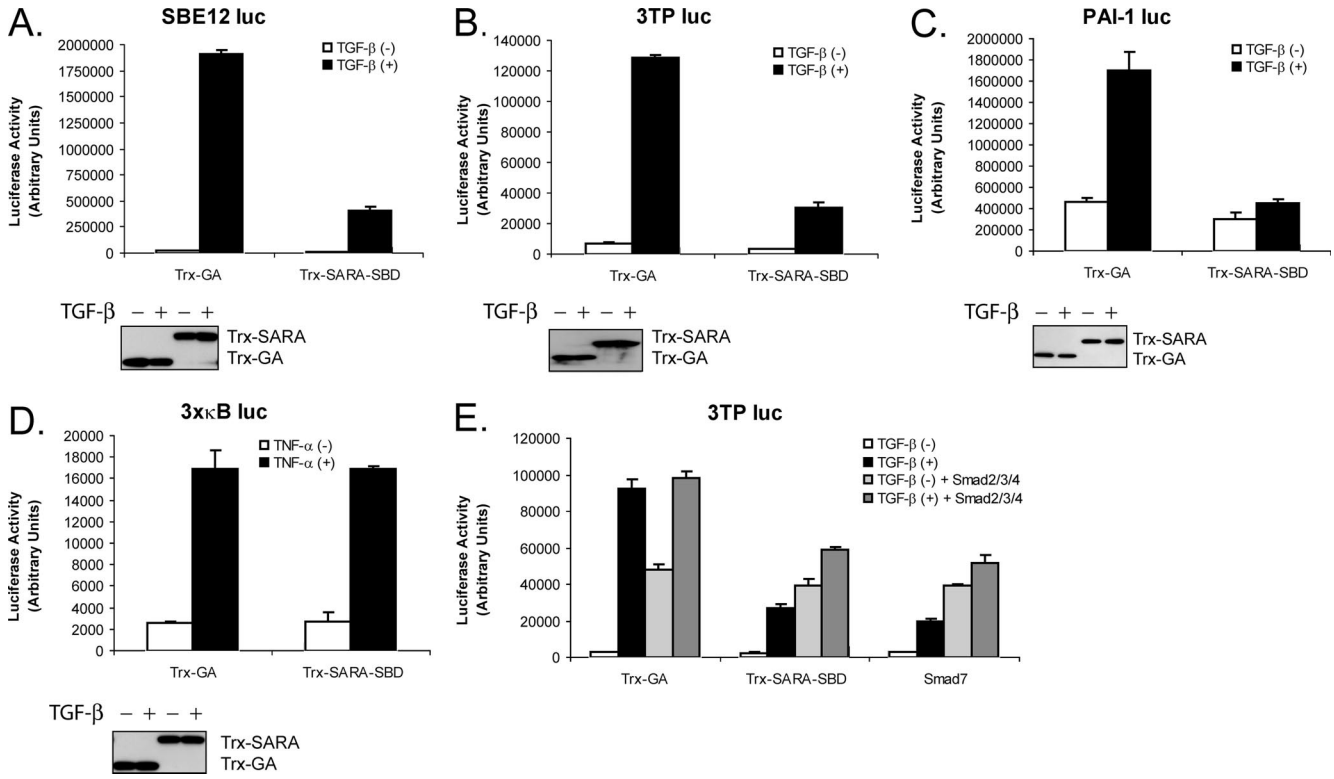

Figure 2. Trx-SARA inhibits TGF-β1–induced gene expression. Cotransfection of an expression construct for Trx-SARA into NMuMG cells inhibited expression from luciferase reporter genes SBE12-luc (A), 3TP-luc (B), and PAI-1-luc (C), but had no effect on the TNF-α reporter gene 3xκB-luc (D). Control transfections used the expression plasmid for Trx-GA. Similar levels of Trx-SARA or Trx-GA were confirmed by Western blotting of total cell lysates to detect the HA-epitope tagged aptamers (panels under each figure). All luciferase assays were normalized to a cotransfected β-galactosidase expression vector to control for transfection efficiency. (E) Overexpression of Smad2, Smad3, and Smad4 rescues the Trx-SARA or Smad7 inhibition of 3TP-luc. Expression plasmids for FLAG -tagged Smad2, Smad3, and Smad4, 0.1 μg of each, were cotransfected with the 3TP-luc reporter gene plasmid into the NMuMG$^{\text{Trx-GA}}$, NMuMG$^{\text{Trx-SARA}}$, and NMuMG$^{\text{Smad7}}$ cell populations. All luciferase assays were normalized to a cotransfected β-galactosidase expression vector to control for transfection efficiency. The overexpressed Smads increased basal activity of the reporter gene to similar levels in all three cell populations. Trx-SARA or Smad7 expression reduced the TGF-β1–induced gene expression. All assays were done in triplicate and SDs are indicated.

Trx-SARA SBD were cotransfected into 293 cells. Cell extracts were immunoprecipitated with anti-Flag antibody, followed by immunoblotting with anti-HA antibody. As shown in Figure 1B, Trx-SARA was detected in the Flag-Smad2 immunoprecipitate. None of the Trx-SARA deletion mutant proteins were detected in the Flag-Smad2 immunoprecipitate, suggesting that the Trx-SARA aptamer required all three structural elements to bind Smad2.

Trx-SARA Aptamer Binds Specifically to Smad2 and Smad3

Eight mammalian Smads have been identified, including Smad1, 5, and 8, the R-Smads in the BMP signaling pathway, and Smad2 and Smad3, the R-Smads in the TGF-β signaling pathway. Smad6 and 7 are inhibitory Smads in the TGF-β– and BMP-signaling pathways. HA-tagged Trx-SARA aptamer was expressed in 293 cells together with different Flag-tagged Smad proteins. Examination of anti-Flag immunoprecipitates by anti-HA westerns indicated that the Trx-SARA protein associated with Smad2 and Smad3 but not Smads 1, 4, or 7 (Figure 1C). A control Trx aptamer, Trx-GA, containing an 11-amino acid repeat of Gly-Ala was not detectable in any of the immunoprecipitates. These data indicate that Trx-SARA maintains the same Smad-binding specificity as full-length SARA (Tsukazaki *et al.*, 1998).

Trx SARA Inhibits TGF-β–responsive Reporter Gene Expression

To determine the transcriptional effects of Trx-SARA, we tested several TGF-β–responsive reporter genes in NMuMG cells. Expression of Trx-SARA greatly reduced the TGF-β–induced luciferase expression from three reporter genes: SBE(CAGA)$_{12}$-luc, 3TP-luc, or PAI-1-luc (Figure 2, A–C). To test the specificity of Trx-SARA inhibition, we also used a non-TGF-β–responsive luciferase reporter, the 3xκB-luc reporter, which is activated by TNF-α treatment (Huang et al., 2000). As shown in Figure 2D, Trx-SARA caused no inhibition of the 3xκb reporter.

To study the effects of Trx-SARA on TGF-β–induced responses in NMuMG cells, we generated retroviral expression vectors that constitutively expressed the aptamers and GFP, or Smad7 and GFP. NMuMG cells were infected with retroviruses encoding Trx-SARA, Trx-GA, or the inhibitory Smad protein, Smad7. High-GFP–expressing cells were recovered by FACS and expanded in culture to provide populations of cells (NMuMG$^{\text{Trx-SARA}}$, NMuMG$^{\text{Trx-GA}}$, and NMuMG$^{\text{Smad7}}$) uniformly expressing the respective aptamer or Smad7. We transiently transfected the 3TP luciferase reporter into these three cell populations and demonstrated that Trx-SARA inhibited TGF-β–induced luciferase activity by 75%, whereas Smad7 inhibited the activity by 85% (Figure 2E). We next examined

whether overexpression of Smad2, Smad3, and Smad4 could rescue the inhibitory effect of Trx-SARA and Smad7 on 3TP-luc reporter activity. As shown in Figure 2E, transfection of Smad2/3/4 increased basal 3TP reporter activity in all three cell populations and increased 3TP-luciferase activity in TGF-β–treated NMuMG$^{Trx\text{-}SARA}$ and NMuMG^{Smad7}cells. The inability of Trx-SARA to inhibit activation of the reporter by the combination of Smad2/Smad3/Smad4 in the absence of ligand-induced phosphorylation of the R-Smads suggests that Trx-SARA may be acting on the phosphorylated R-Smads or the trimeric complex formed by phosphorylated R-Smads.

Trx-SARA Inhibits TGF-β–induced EMT

TGF-β induces EMT, which comprises loss of epithelial cell morphology, dissociation of cell–cell contacts, reduction in proteins mediating cell–cell contacts, remodeling of the actin cytoskeleton, and acquisition of an elongated, mesenchymal cell shape (Thiery, 2002, 2003). In normal development, EMT has been associated with processes in gastrulation, heart formation, somitogenesis, palate formation, and Mullerian tract regression (Savagner, 2001; Shook and Keller, 2003). EMT has been causally linked to tumor invasion and metastasis (Gotzmann *et al.,* 2004). In renal fibrosis, tubular epithelial cells undergo EMT in response to primary insults such as hypertension or diabetes, which results in the production and deposition of extracellular matrix proteins (Zeisberg and Kalluri, 2004). Multiple signaling proteins have been implicated in the induction of EMT by TGF-β, including Ras/MAPK (Oft *et al.,* 1996, 1998, 2002), integrin β-1 (Bhowmick *et al.,* 2001a), integrin-linked kinase (Li *et al.,* 2003b), p38MAPK (Bakin *et al.,* 2002), Rho kinase (Bhowmick *et al.,* 2001b), phosphatidylinositol 3 (PI3)-kinase (Bakin *et al.,* 2000), Jagged1/Notch (Zavadil *et al.,* 2004), and NF-κB (Huber *et al.,* 2004). The Smad proteins are also important for the EMT response as demonstrated by studies on Smad2 (Oft *et al.,* 2002), overexpression of Smad2 or Smad3 with Smad4 (Piek *et al.,* 1999), use of a type I receptor mutant that is unable to phosphorylate R-Smads (Itoh *et al.,* 2003), use of conditional Smad4 knockout mice (Li *et al.,* 2003a), use of Smad3 knockout mice (Sato *et al.,* 2003; Saika *et al.,* 2004; Zavadil *et al.,* 2004), and use of dominant negative Smads (Valcourt *et al.,* 2005).

TGF-β–induced EMT in NMuMG cells was assayed by the morphological change of the cells and by a number of well-characterized molecular changes. We used the cell populations generated by retroviral infection and cell sorting for GFP expression to test the effect of the aptamers on the EMT response in NMuMG cells. In the control NMuMG$^{Trx\text{-}GA}$ cells, treatment with 100 pM TGF-β for 24 h induced cells to change shape from a cobblestone-like appearance of epithelial cell morphology to a more elongated mesenchymal cell morphology; this morphological change was more apparent at 48 h (Figure 3A). Neither NMuMG$^{Trx\text{-}SARA}$ nor NMuMG^{Smad7} cells changed morphology in response to TGF-β (Figure 3A). To verify that Trx-SARA and Smad7 expression in NMuMG cells blocked TGF-β–induced EMT, we examined several epithelial and mesenchymal molecular markers in the cells. As shown in Figure 3B, NMuMG$^{Trx\text{-}GA}$ cells treated with 100 pM TGF-β for 48 h lost E-cadherin staining. In contrast, the epithelial cell marker E-cadherin was detected at the junctions between neighboring NMuMG$^{Trx\text{-}SARA}$ cells even in the presence of 100 pM TGF-β (Figure 3B). NMuMG^{Smad7} cells showed discontinuous and diffuse E-cadherin staining at the cell–cell junction. We also examined stress fiber formation by phalloidin staining and the expression pattern of vimentin. As shown in Figure 3B, F-actin distribution was mainly at the cell–cell borders and no stress fibers were observed in non-TGF-β–treated cells. However, when cells were treated with TGF-β for 48 h, the F-actin distribution changed, and stress fibers were formed throughout NMuMG$^{Trx\text{-}GA}$ cells. In contrast, NMuMG$^{Trx\text{-}SARA}$ and NMuMG^{Smad7} cells did not exhibit mesenchymal patterns of phalloidin or vimentin straining (Figure 3B). Western blot analysis was performed to analyze the expression level of E- and N-cadherin. As shown in Figure 3C, E-cadherin levels decreased, whereas N-cadherin increased in NMuMG$^{Trx\text{-}GA}$ cells in response to TGF-β treatment. In contrast, there was no detectable change in E- or N-cadherin levels in NMuMG cells expressing Trx-SARA or Smad7. Western analysis confirmed that the NMuMG$^{Trx\text{-}SARA}$ and NMuMG$^{Trx\text{-}GA}$ cell populations expressed similar levels of HA-tagged Trx protein (Figure 3C).

Trx-SARA Impairs Smad Phosphorylation Only at the Earliest Time Point

To determine if expression of Trx-SARA blocked TGF-β–induced phosphorylation of Smad2 and Smad3, we analyzed the phosphorylated Smad2 and Smad3 level in the three cell populations: NMuMG$^{Trx\text{-}GA}$, NMuMG$^{Trx\text{-}SARA}$ and NMuMG^{Smad7} (Figure 4). Western blot analysis of total cell lysates from NMuMG$^{Trx\text{-}GA}$ and NMuMG$^{Trx\text{-}SARA}$ cells indicated a reduced level of phospho-Smad2 protein in NMuMG$^{Trx\text{-}SARA}$ cells 15 min after addition of 100 pM TGF-β (Figure 4A). By 30 min after TGF-β addition, however, the levels of phospho-Smad were similar in both cell populations, and this similarity was maintained through the 24-h time course (Figures 4, A and B). By contrast, expression of Smad7 in NMuMG cells decreased levels of phosphorylated Smad2 and Smad3 (Figure 4B).

Trx-SARA Does Not Impair ERK/MAPK, p38, or Akt Phosphorylation

p38 mitogen–activated protein kinase (Bhowmick *et al.,* 2001a), the phosphoinositide-3′kinase, Akt (Bakin *et al.,* 2000), and the ERK/MAPK (Xie *et al.,* 2004) also contribute to TGF-β–induced EMT in NMuMG cells. Treatment with TGF-β for 1 or 2 h moderately increased phosphorylation of Erk/MAPK, p38MAPK, and Akt in NMuMG$^{Trx\text{-}GA}$ cells (Figure 4C), and these increases were not altered by expression of Trx-SARA. Reduced TGF-β–induced phosphorylation of p42/44 ERK/MAPK and higher phosphorylation of p38 and Akt were observed in NMuMG^{Smad7} cells. The increased phosphorylation of p38 is in agreement with reports that Smad7 can serve as a scaffold for assembly of kinases that activate p38 kinase (Edlund *et al.,* 2003). Phosphorylation of ERK/MAPK p42/44 or p38MAPK by EGF or osmotic shock, respectively, were not altered in the NMuMG$^{Trx\text{-}SARA}$ and NMuMG^{Smad7} cells (Figure 4, D and E).

Trx SARA Inhibits Smad2/3 Nucleocytoplasmic Shuttling

Smad2 and Smad3 are continually shuttling between the nucleus and cytoplasm even in their nonphosphorylated state (Inman *et al.,* 2002b; Xu *et al.,* 2002). A previous study demonstrated that overexpression of a fragment of SARA prevented Smad2 nuclear import into isolated nuclei by masking the nuclear import signal of Smad2 (Xu *et al.,* 2000). Trx-SARA and the control aptamer, Trx-GA, were both predominantly localized in the nucleus of the NMuMG cell populations by immunostaining for the HA-epitope tag (Figure 5A). In the nonstimulated NMuMG$^{Trx\text{-}GA}$ cells, Smad2 (Figure 5B) and Smad3 (Figure 5C) were distributed in both the cytoplasm and the nucleus. After TGF-β stimulation, Smad2 and Smad3 were localized predominantly in the nucleus, consistent with normal Smad protein translocation in the Trx-GA cell population (Figure 5, B and C). In con-

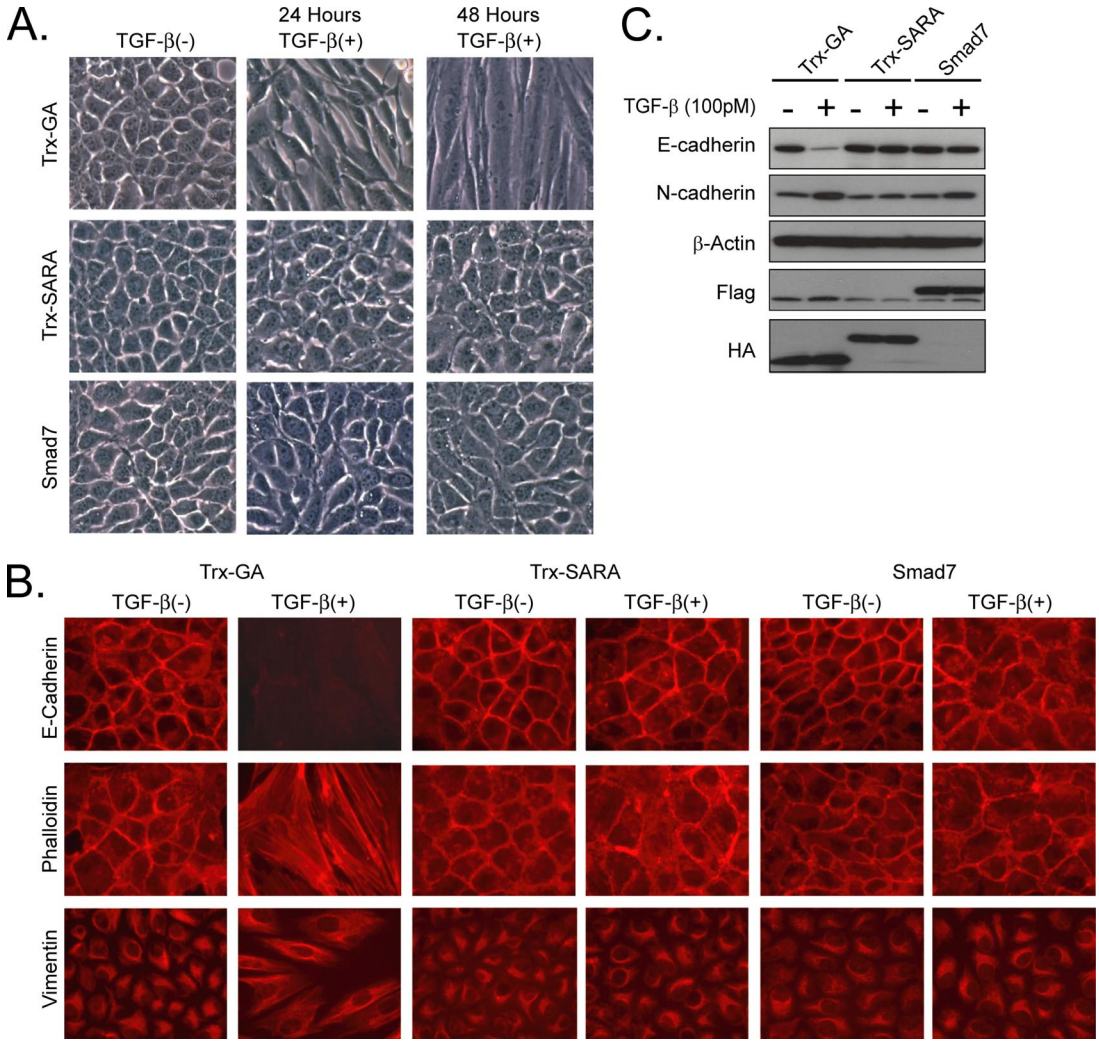

Figure 3. Stable expression of the peptide aptamer Trx-SARA or Smad7 in NMuMG cells inhibits TGF-β–induced EMT. (A) Phase-contrast images of NMuMG$^{Trx\text{-}GA}$, NMuMG$^{Trx\text{-}SARA}$, and NMuMG^{Smad7} cells treated with TGF-β1 (100 pM) for 24 or 48 h. The transition between cobblestone epithelial morphology to spindle-shaped mesenchymal morphology is observed only in NMuMG$^{Trx\text{-}GA}$ cells. (B) E-cadherin, phalloidin, and vimentin staining of the NMuMG$^{Trx\text{-}GA}$, NMuMG$^{Trx\text{-}SARA}$, and NMuMG^{Smad7} cells in the presence or the absence of TGF-β1 (100 pM) for 48 h. The epithelial marker E-cadherin decreased and phalloidin-stained actin stress fibers formed in NMuMG$^{Trx\text{-}GA}$ cells, but these changes were not observed in NMuMG$^{Trx\text{-}SARA}$ or NMuMG^{Smad7} cells. Vimentin staining was also unchanged in NMuMG$^{Trx\text{-}SARA}$ or NMuMG^{Smad7} cells. (C) Analysis of endogenous E- and N-cadherin protein levels in NMuMG$^{Trx\text{-}GA}$, NMuMG$^{Trx\text{-}SARA}$, and NMuMG^{Smad7} cells. Lysates from cells untreated or treated for 48 h with TGF-β1 were resolved by SDS-PAGE and analyzed by Western blotting. Equivalent loading was confirmed by detecting β-actin. Similar levels of control and Trx-SARA aptamer were confirmed by detecting the HA-epitope tag. Expression of the Flag-Smad7 was confirmed by detecting the Flag-epitope tag. Both Trx-SARA and Smad7 blocked TGF-β–induced reduction in E-cadherin expression.

trast, Smad2 and Smad3 were localized in the nucleus in NMuMG$^{Trx\text{-}SARA}$ cells even without TGF-β stimulation (Figure 5, B and C). Treatment of NMuMG$^{Trx\text{-}SARA}$ cells with TGF-β only slightly increased Smad2 and Smad3 nuclear levels. In the NMuMG^{Smad7} cells, the Smad2 and Smad3 cellular localization was cytoplasmic, similar to GA cells in the absence of TGF-β (Figure 5, B and C). When NMuMG^{Smad7} cells were treated with TGF-β, there was much less nuclear Smad2 or Smad3 staining detected, indicating that nuclear accumulation of Smad2 or Smad3 is reduced; this is consistent with the reduced Smad2 and Smad3 phosphorylation in NMuMG^{Smad7}cells (Figure 4A). Smad 4 shuttles into and out of the nucleus independently from the R-Smads (Inman *et al.*, 2002b; Xu *et al.*, 2002). Because Trx-SARA does not bind to Smad4, the cellular distribution of Smad4 should not be altered in Trx-SARA expressing cells. Immunohistochemical detection of Smad4 revealed no differences in the distribution of Smad4 between NMuMG$^{Trx\text{-}GA}$ and NMuMG$^{Trx\text{-}SARA}$ cells (Figure 5D).

To validate the immunohistochemical observations, subcellular fractionation experiments were also performed using cell populations of NMuMG$^{Trx\text{-}GA}$, NMuMG$^{Trx\text{-}SARA}$, and NMuMG^{Smad7}(Figure 5E). The accumulation of Smad 3 in the nuclear fraction after TGF-β treatment was detected in the NMuMG$^{Trx\text{-}GA}$ cell fractions. In agreement with the immunohistochemical data, Smad3 was found predominantly in the nuclear fraction of NMuMG$^{Trx\text{-}SARA}$ cells even without TGF-β treatment, and treatment of TGF-β did not increase Smad3 in the nuclear fraction (Figure 5E). Although Trx-SARA apparently impedes nuclear export, leading to

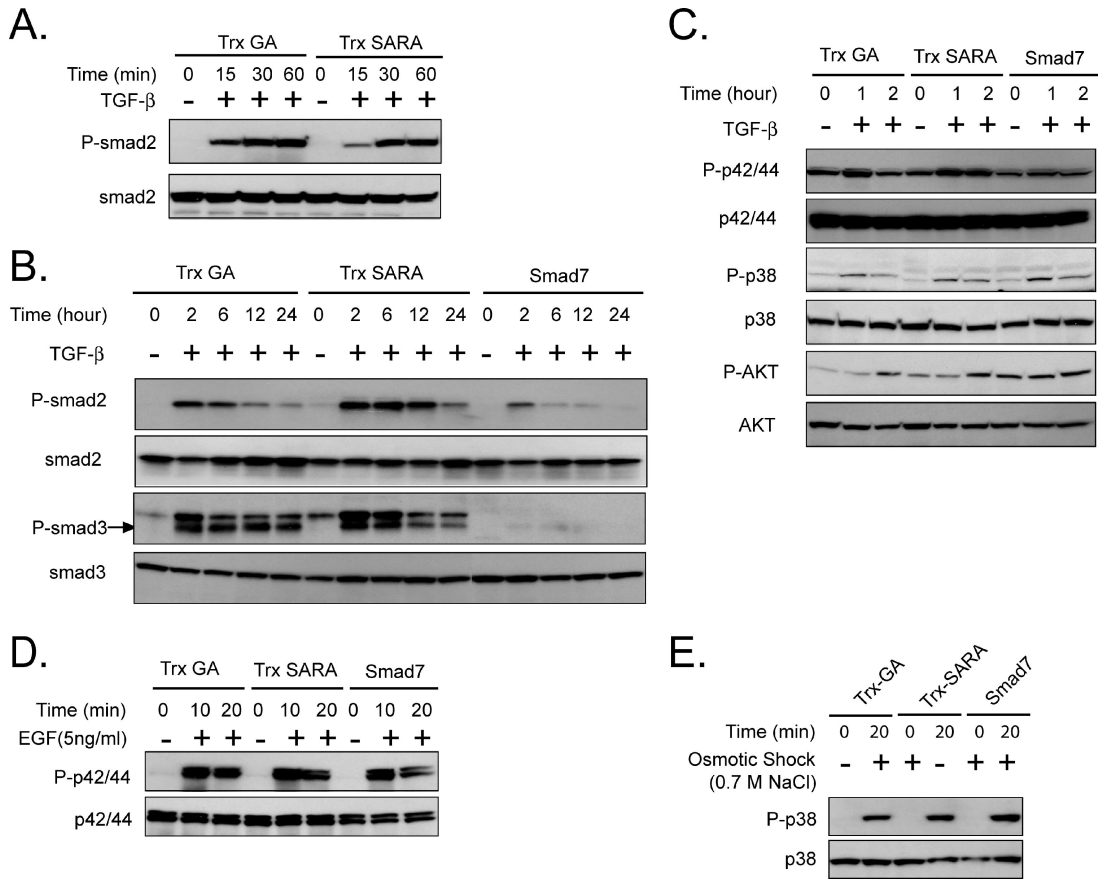

Figure 4. Trx-SARA interferes with the initial phosphorylation of Smad but does not interfere with other changes in protein phosphorylation induced by TGF-β, EGF, or osmotic shock in NMuMG cells. (A) NMuMG$^{Trx\text{-}GA}$ and NMuMG$^{Trx\text{-}SARA}$ cells were treated with 100 pM TGF-β1 for 0, 15, 30, or 60 min, total cell lysates were prepared, resolved by SDS-PAGE, and analyzed for total Smad2 and phospho-Smad2 using specific antibodies. The level of phospho-Smad2 was reduced only at the 15-min time point. (B) NMuMG$^{Trx\text{-}GA}$, NMuMG$^{Trx\text{-}SARA}$, and NMuMG^{Smad7} cells were treated with 100 pM TGF-β1 for 0, 2, 6, 12, or 24 h, total cell lysates were prepared, resolved by SDS-PAGE, and analyzed for total Smad2, total Smad3, phospho-Smad2, or phospho-Smad3 (lower band, arrow) using specific antibodies. Only Smad7–expressing cells had diminished levels of phospho-Smads. The higher levels of pSmad2 or pSmad3 in Trx-SARA compared with Trx-GA cells in this figure have not been reproducible. (C) Western blot analysis of TGF-β–induced phosphorylation of Erk1/2, p38MAPK, and Akt in NMuMG$^{Trx\text{-}GA}$, NMuMG$^{Trx\text{-}SARA}$, and NMuMG^{Smad7} cells. Cells were treated or not treated with 100 pM TGF-β1 for 1 or 2 h, total cell lysates were prepared, resolved by SDS-PAGE, and subject to immunoblotting using antibodies against phosphorylated p42/44 ERK/MAPK, total ERK/MAPK, phospho-Akt, total Akt, phospho-p38MAPK, and total p38MAPK. TGF-β–induced increases in the phosphorylation of all three proteins were observed in both NMuMG$^{Trx\text{-}GA}$ and NMuMG$^{Trx\text{-}SARA}$ cells. The NMuMG^{Smad7} cells had reduced phosphorylation of p42/44 ERK/MAPK and higher phosphorylation levels of p38MAPK and Akt. (D) EGF-induced Erk1/2 phosphorylation was not blocked in NMuMG$^{Trx\text{-}GA}$, NMuMG$^{Trx\text{-}SARA}$, or NMuMG^{Smad7} cells. (E) Osmotic shock–induced p38 phosphorylation was not affected in NMuMG$^{Trx\text{-}GA}$, NMuMG$^{Trx\text{-}SARA}$, or NMuMG^{Smad7} cells. The much less intense bands for phospho-p42/44 or phospho-p38 at zero time in D and E, respectively, compared with C, are due to the much shorter exposure times used for D and E.

high levels of nuclear R-Smads in the absence of TGF-β, the normal phosphorylation levels of Smad2 and Smad3 in response to TGF-β stimulation of Trx-SARA cells (Figure 4 A and B) indicate that nuclear-cytoplasmic shuttling still occurs in the Trx-SARA cells because the Smads must have access to the cell surface receptors to maintain the phosphorylated state (Inman *et al.,* 2002b; Xu *et al.,* 2002). When compared with the control cells after TGF-β stimulation, the TGF-β–stimulated Trx-SARA cells contain comparable levels of phosphorylated R-Smad and comparable levels of total nuclear R-Smad. Therefore, the ability of Trx-SARA to inhibit TGF-β–induced reporter genes and EMT is not explained by the altered basal subcellular localization of the R-Smads.

Trx-SARA Impairs Smad3–Smad4 Complex Formation

The assembly of phosphorylated Smad2 into a trimeric complex results in a 12 Å conformational change in the Smad MH2 domain that reduces binding to SARA through disruption of the β-sheet formed between the beta strand in SARA and the N-terminal β1′-strand of the MH2 domain (Wu *et al.,* 2000). This conformational change facilitates the Smad–Smad interface binding in the heterotrimeric complexes comprising Smad4 and phosphorylated Smad2 or Smad3. Previous studies have shown that Smad2 could bind either SARA or Smad4 but not both proteins together, suggesting mutually exclusive binding of SARA and Smad4 by the two different conformations of Smad2 (Tsukazaki *et al.,* 1998). We tested whether expression of Trx-SARA in NMuMG cells disrupts the Smad2–Smad4 or Smad3–Smad4 complexes. NMuMG$^{Trx\text{-}GA}$, NMuMG$^{Trx\text{-}SARA}$, and NMuMG^{Smad7} cells were treated with or without TGF-β for 2 h, and cell lysates were immunoprecipitated with anti-Smad2 or anti-Smad3 antibodies. Immunoprecipitated Smad2 (Figure 6A) or Smad3 (Figure 6B) protein complexes were analyzed by

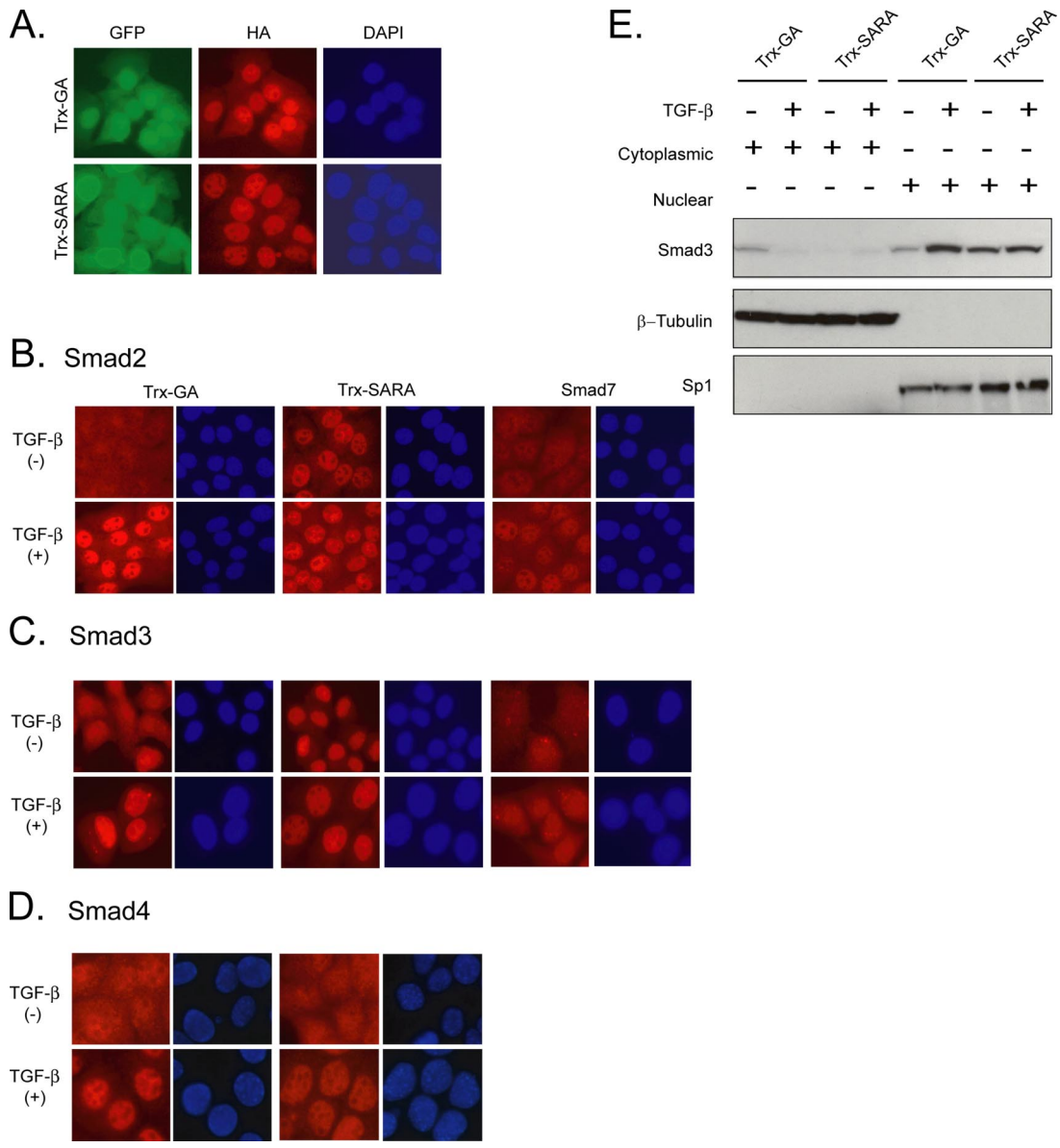

Figure 5. Trx SARA expression alters the basal distribution of Smad2 and Smad3 but not Smad 4 in the cell. (A) HA-epitope–tagged peptide aptamers Trx-GA and Trx-SARA were detected by anti-HA immunohistochemistry predominantly in the nucleus. The GFP expressed from the integrated proviral vector was distributed more equally in both the nucleus and cytoplasm. Nuclei were detected by DAPI staining. (B and C) Immunohistochemical localization detected Smad2 (B) and Smad3 (C) in NMuMG$^{Trx\text{-}GA}$, NMuMG$^{Trx\text{-}SARA}$, and NMuMG^{Smad7} cells. Cells were treated with or without TGF-β1 (100 pM) for 90 min, fixed with 4% paraformaldehyde, and stained for Smad2 (red), Smad3 (red), or DNA (DAPI, blue). In NMuMG$^{Trx\text{-}GA}$ cells, TGF-β1 caused the expected accumulation of both Smads in the nucleus. In NMuMG$^{Trx\text{-}SARA}$ cells, however, the Smads were predominantly in the nucleus even without TGF-β1 treatment. The NMuMG^{Smad7} cells exhibited lower levels of nuclear Smad 2 or Smad3 after TGF-β1 stimulation. (D) Immunohistochemical localization of Smad4 in NMuMG$^{Trx\text{-}GA}$ and NMuMG$^{Trx\text{-}SARA}$ cells. Cells were treated with or without TGF-β1 (100 pM) for 90 min, fixed with 4% paraformaldehyde, and stained for Smad4 (red) or DNA (DAPI, blue). In contrast to the basal nuclear localization of Smad2 and Smad3 in NMuMG$^{Trx\text{-}SARA}$ cells, Smad4 was observed in both nucleus and cytoplasm of nonstimulated NMuMG$^{Trx\text{-}GA}$ and NMuMG$^{Trx\text{-}SARA}$ cells. TGF-β1 caused accumulation of Smad4 in the nucleus in both cell populations. (E) Nuclear and cytoplasmic fractions of the cells were prepared to confirm the subcellular localization of Smad3. Cells were untreated or treated with TGF-β for 2 h, and nuclear extracts and cytoplasmic fractions were prepared, resolved by SDS-PAGE, and analyzed by Western blotting. Detection of tubulin and Sp1 were used to confirm the separation of the nuclear and cytoplasmic fractions and the equivalent loading of each sample. Smad 3 was present in both cytoplasmic and nuclear fractions in unstimulated NMuMG$^{Trx\text{-}GA}$ cells but was detected only in the nuclear fraction of stimulated cells. In the NMuMG$^{Trx\text{-}SARA}$ cells, most of the detectable Smad3 was present only in the nuclear fraction of either unstimulated or TGF-β–stimulated cells.

Western blot analysis using anti-Smad4 antibody. TGF-β treatment increased Smad2/4 and Smad3/4 complex formation in NMuMG$^{Trx\text{-}GA}$ cells. We observed lower levels of Smad2/4 (Figure 6A) and Smad3/4 (Figure 6B) in NMuMG$^{Trx\text{-}SARA}$ cells, suggesting that the interactions between endogenous Smad4 with Smad2 or Smad3 were disrupted by the binding of Trx-SARA to Smad2 or Smad3. Consistent with this ability to disrupt or reduce the formation of R-Smad-Smad4

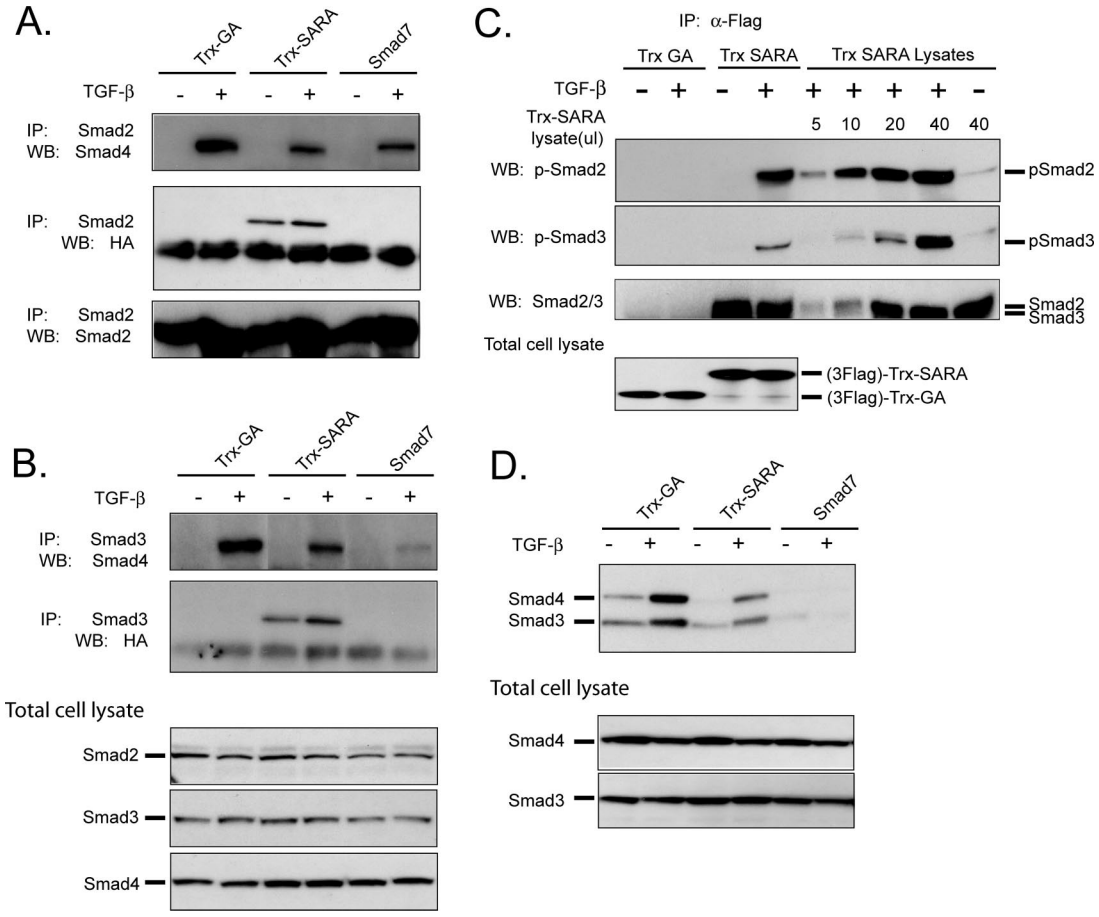

Figure 6. Trx SARA disrupts Smad2/4 or Smad3/4 protein complexes after TGF-β stimulation. (A and B) Cells were treated with or without TGF-β for 2 h and then lysed with TNE buffer. The same amount of cell lysate from NMuMG$^{Trx\text{-}GA}$, NMuMG$^{Trx\text{-}SARA}$, and NMuMG^{Smad7} cells was used for immunoprecipitation with Smad2 (A) or Smad3 (B) antibody. Immunoprecipitates were blotted with anti-Smad4 (top panel), anti-HA (middle panel) and anti-Smad2 or anti-Smad3 (bottom panel). The amount of TGF-β–induced complex with Smad4 was reduced in NMuMG$^{Trx\text{-}SARA}$ and NMuMG^{Smad7} cells. The HA epitope–tagged Trx-SARA aptamer was detected at similar levels in the immunoprecipitates of endogenous Smad2 or Smad3 from NMuMG$^{Trx\text{-}SARA}$ cells, regardless of whether the cells had been treated with TGF-β. (C) Plasmids expressing Flag-tagged Trx-GA or Trx-SARA were transfected into NMuMg cells. After 24 h, cells were treated with TGF-β for 2 h and lysed. Anti-Flag antibody immunoprecipitates (from 500 μl of lysates) or aliquots of lysates were resolved by SDS-PAGE and examined by Western blotting for endogenous phospho-Smad2, endogenous phospho-Smad3, endogenous total Smad2 and Smad3, or Flag-tagged aptamer. The Trx-GA and Trx-SARA aptamers were expressed at similar levels; however, the Trx-GA immunoprecipitate contained no detectable Smad2. The Trx-SARA immunoprecipitate from TGF-β– treated cells, contained Smad2, Smad3, phospho-Smad2, and phospho-Smad3 at levels similar to 20 μl of total lysate. (D) A Smad-binding biotinylated oligonucleotide, SBE4, was added to the cell lysates from NMuMG$^{Trx\text{-}GA}$, NMuMG$^{Trx\text{-}SARA}$, and NMuMG^{Smad7} cells and recovered with Streptavidin beads. The total cell lysates and the eluted proteins were analyzed by Western blotting with anti-Smad3 and anti-Smad4. The amount of TGF-β–induced Smad3-Smad4 complex bound to DNA was reduced in NMuMG$^{Trx\text{-}SARA}$ and NMuMG^{Smad7} cells.

trimers, the Trx-SARA aptamer immunoprecipitated either total Smad2 and 3 or phospho-Smad2 and 3 at similar efficiencies from cell lysates (Figure 6C). Because most of the detectable R-Smad is in the nucleus of NMuMG$^{Trx\text{-}SARA}$ cells (Figure 5), the immunoprecipitates from NMuMG$^{Trx\text{-}SARA}$ cells examined primarily the association of nuclear R-Smad with Smad4. Although the Smad2 and Smad3 immunoprecipitates from NMuMG$^{Trx\text{-}SARA}$ cells contained less Smad4 protein, they did contain detectable Trx-SARA, indicating association of the aptamer with endogenous Smad2 and Smad3. The amounts of Trx-SARA in the immunoprecipitates from nonstimulated or TGF-β–stimulated NMuMG$^{Trx\text{-}SARA}$ cells were similar, even though the TGF-β–treated NMuMG$^{Trx\text{-}SARA}$ cells contain normal amounts of phosphorylated R-Smads (Figure 4). NMuMG^{Smad7}cells also exhibited a significant decrease in the amount of Smad2 and Smad3 in Smad4 complexes, but this was expected because of the reduced Smad2 and Smad3 phosphorylation in NMuMG^{Smad7}cells (Figure 4).

The Smad2 and Smad3 complexes with Smad4 bind to DNA to regulate gene expression. We tested whether the binding of Smad3–Smad4 complex to the Smad binding element was altered in the cell populations using an oligonucleotide pull-down assay (Figure 6D). TGF-β caused a significant increase in Smad3 and Smad4 from NMuMG$^{Trx\text{-}GA}$ cell lysates bound to the Smad-binding element DNA. The level of complex that bound to Smad-binding element DNA in cell lysates from NMuMG$^{Trx\text{-}SARA}$ or NMuMG^{Smad7}cells was reduced. The level of Smad complex in cell lysates from TGF-β–treated NMuMG$^{Trx\text{-}SARA}$ cells that bound to DNA was similar to the basal level of DNA-bound complex from untreated NMuMG$^{Trx\text{-}GA}$ cells.

DISCUSSION

The ability of the Trx-SARA peptide aptamer to inhibit TGF-β activation of gene expression and induction of EMT demonstrates that peptide aptamers can be expressed at sufficient levels and with sufficient protein binding affinity to perturb R-Smad function in living cells. Generation of peptide aptamers that bind other sites on R-Smads should be a useful strategy for determining which protein-binding sites on R-Smads are required for specific responses to TGF-β. Previous studies using overexpression of Smad7 or dominant negative Smads have produced conflicting conclusions on the importance of the endogenous Smads for EMT in NMuMg cells (Bhowmick *et al.*, 2001b; Valcourt *et al.*, 2005); the results reported here with the Trx-SARA peptide aptamer provide further support that Smad2 and Smad3 are required for TGF-β–induced EMT in NMuMg cells.

Smad2 and Smad3 nuclear import and export are mediated by phenylalanine-glycine-repeat–containing nucleoporins such as CAN/Nup214 and Nup153 and do not require Smad phosphorylation, importin-α, or importin-β (Xu *et al.*, 2000, 2002, 2003). The nucleoporins bind the "hydrophobic corridor" in the Smad MH2 domain (Xu *et al.*, 2002, 2003). Nuclear import of Smad2 or Smad3 in an in vitro assay was inhibited by binding of the SARA SBD to hydrophobic corridor and nuclear export was inhibited by overexpression of the FoxH1 transcription factor, which also binds hydrophobic corridor (Hoodless *et al.*, 1999; Xu *et al.*, 2000, 2002, 2003). Missense mutations in the Smad hydrophobic corridor have no effect on the levels of TGF-β–induced Smad phosphorylation or Smad2 association with Smad4 but block nuclear import and thereby reduce the activation of TGF-β–responsive reporter gene expression (Xu *et al.*, 2002, 2003). In the absence of TGF-β, most of the cellular pool of Smad2 and Smad3 is located in the cytoplasm. This distribution may be the result of Smad association with cytoplasmic retention proteins such as SARA (Tsukazaki *et al.*, 1998), microtubules (Dong *et al.*, 2000), or filamin (Sasaki *et al.*, 2001) or simply may be due to a more rapid rate of nuclear export than import (Schmierer and Hill, 2005). TGF-β–induced phosphorylation of Smad proteins results in their accumulation in the nucleus in approximately 30 min. When TGF-β receptor activity is terminated, the Smads return to a predominantly cytoplasmic localization in about 2 h (Inman *et al.*, 2002b). The Trx-SARA aptamer caused the subcellular distribution of Smad2 and Smad3, but not Smad4, to change from primarily cytoplasmic to primarily nuclear. We believe the pools of R-Smads accumulate in the nucleus because binding of the Trx-SARA aptamer to the two R-Smads impedes nuclear export. Trx-SARA, and Trx-GA contain NLS sequences and, by immunohistochemical staining, are preferentially enriched in the nucleus of the NMuMG cells. The higher concentrations of Trx-SARA in the nucleus should be more effective in inhibiting Smad export than lower amounts of cytoplasmic Trx-SARA are in impeding Smad import.

Although the Trx-SARA aptamer alters the subcellular location of the Smad2 and 3 pools, this does not alter the levels of phosphorylated Smads generated by receptor activation, except at the earliest time point 15 min after TGF-β addition, indicating there are sufficient cytoplasmic pools of Smad2 and Smad3 to interact with receptor. This is analogous to the finding that during TGF-β signaling most of the detectable Smad2 is located in the nucleus within 30 min after addition of TGF-β, but there is sufficient nucleocytoplasmic shuttling of Smad to sustain on-going rephosphorylation by activated receptor (Inman *et al.*, 2002b). If nuclear export of Smad was completely blocked by Trx-SARA, there should be reduced levels of cytoplasmic Smad available to the receptor and reduced levels of phosphorylated Smad when cells are treated with TGF-β. The temporary lower level of phospho-Smad protein observed 15 min after TGF-β addition may be caused by the initially lower levels of cytoplasmic R-Smads in the Trx-SARA–expressing cells and/or the nuclear export rate providing a rate-limiting step. Although we cannot rule out that lower level of phospho-Smad at 15 min may contribute to some of the biological effect in Trx-SARA cells, this seem unlikely in that sustained R-Smad activation of several hours is needed to generate biological responses (Inman *et al.*, 2002b; Nicolas and Hill, 2003). The observation that Smad phosphorylation levels are maintained in Trx-SARA cells over the same time course as in control cells also argues that there must be sufficient nuclear export of Smads for rephosphorylation by the active receptors. The activity state of the receptor is monitored by a continual process of Smad de-phosphorylation, export to the cytoplasm, rephosphorylation by the active receptors, nuclear import, and reassembly of active Smad heterotrimers with Smad4 (Inman *et al.*, 2002b). Therefore alteration in the basal subcellular location of the R-Smad pools does not appear to be the cause of inhibition of TGF-β–activated reporter gene expression and EMT by Trx-SARA.

The level of Smad2–Smad4 and Smad3–Smad4 complexes formed after TGF-β stimulation was significantly reduced in cells expressing Trx-SARA. This was also true in cells expressing Smad7, but in those cells the levels of phosphorylated Smad proteins were greatly reduced, and nonphosphorylated Smad proteins do not form a complex with Smad4. Reduction in the level of the Smad2–Smad4 complex or the Smad3–Smad4 complex would be expected to impede gene expression responses to TGF-β because the heterocomplexes are the form of Smad that participate in transcriptional regulatory complexes. Previous work has established that binding of SARA or Smad4 to Smad2 is mutually exclusive and the structural basis for this has been correlated with the two different conformations of R-Smad bound to SARA or bound to Smad4. The SARA binding site is available on the surface of the trimer and is not physically occluded by the trimer interactions (Qin *et al.*, 2002). Both phosphorylated and nonphosphorylated Smad proteins bind to Trx-SARA in coimmunoprecipitation experiments, and binding of the SARA SBD to a trimeric phospho-Smad3 protein caused the trimeric protein to dissociate into monomers (Qin *et al.*, 2002). The prior work on Smad-SARA interactions are consistent with a mechanism in which high levels of Trx-SARA in the nucleus bind to phospho-Smad2 or phospho-Smad3 in the heterotrimeric complex and drive the conformation of the Smad to a SARA-binding state, thereby dissociating the phospho-R-Smad from the Smad4 complex. This would lead to the observed reduced levels of Smad2–Smad4 and Smad3–Smad4 complexes in Trx-SARA cells and reduce Smad-dependent transcriptional responses to TGF-β. This distinct mechanism of Smad inhibition by Trx-SARA should avoid interference with Smad-independent functions of the TGF-β receptors and should have a more selective inhibitory effect on TGF-β signaling than overexpression of Smad7. We have not ruled out that Trx-SARA may also compete for the binding with another critical nuclear factor required for transcriptional activity by R-Smads. The ability of Trx-SARA to block the induction of EMT in mammary epithelial cells in culture demonstrates that this peptide aptamer can be used to explore the roles of TGF-β–induced Smad-dependent signaling in normal physiology and disease.

ACKNOWLEDGMENTS

We are grateful to Drs. Joan Massagué, Peter ten Dijke, Shigeki Miyamoto, and Rik Derynck for expression constructs and luciferase reporter constructs and Dr. Ed Leof for antibody to phospho-Smad3. This work was supported by National Cancer Institute Grant R01 CA090875 to F.M.H. and Cancer Center Support Grant P30 CA014520. B.Z. was supported by the predoctoral training grant in Cancer Biology T32-CA09135.

REFERENCES

Bai, S., and Cao, X. (2002). A nuclear antagonistic mechanism of inhibitory Smads in transforming growth factor-beta signaling. J. Biol. Chem. *277*, 4176–4182.

Bakin, A. V., Rinehart, C., Tomlinson, A. K., and Arteaga, C. L. (2002). p38 mitogen-activated protein kinase is required for TGFbeta-mediated fibroblastic transdifferentiation and cell migration. J. Cell Sci. *115*, 3193–3206.

Bakin, A. V., Tomlinson, A. K., Bhowmick, N. A., Moses, H. L., and Arteaga, C. L. (2000). Phosphatidylinositol 3-kinase function is required for transforming growth factor beta-mediated epithelial to mesenchymal transition and cell migration. J. Biol. Chem. *275*, 36803–36810.

Bandyopadhyay, A., Lopez-Casillas, F., Malik, S. N., Montiel, J. L., Mendoza, V., Yang, J., and Sun, L. Z. (2002). Antitumor activity of a recombinant soluble betaglycan in human breast cancer xenograft. Cancer Res. *62*, 4690–4695.

Bhowmick, N. A., Zent, R., Ghaissi, M., McDonnell, M., and Moses, H. L. (2001a). Integrin β1 signaling is necessary for transforming growth factor-β activation of p38MAPK and epithelial plasticity. J. Biol. Chem. *276*, 46707–46713.

Bhowmick, N. A., Ghiassi, M., Bakin, A., Aakre, M., Lundquist, C. A., Engel, M. E., Arteaga, C. L., and Moses, H. L. (2001b). Transforming growth factor-beta1 mediates epithelial to mesenchymal transdifferentiation through a RhoA-dependent mechanism. Mol. Biol. Cell *12*, 27–36.

Bottger, A., Bottger, V., Sparks, A., Liu, W. L., Howard, S. F., and Lane, D. P. (1997). Design of a synthetic Mdm2-binding mini protein that activates the p53 response in vivo. Curr. Biol. *7*, 860–869.

Buerger, C., Nagel-Wolfrum, K., Kunz, C., Wittig, I., Butz, K., Hoppe-Seyler, F., and Groner, B. (2003). Sequence-specific peptide aptamers, interacting with the intracellular domain of the epidermal growth factor receptor, interfere with Stat3 activation and inhibit the growth of tumor cells. J. Biol. Chem. *278*, 37610–37621.

Cohen, B. A., Colas, P., and Brent, R. (1998). An artificial cell-cycle inhibitor isolated from a combinatorial library. Proc. Natl. Acad. Sci. USA *95*, 14272–14277.

Colas, P., Cohen, B., Jessen, T., Grishina, I., McCoy, J., and Brent, R. (1996). Genetic selection of peptide aptamers that recognize and inhibit cyclin- dependent kinase 2. Nature *380*, 548–550.

Cui, Q., Lim, S. K., Zhao, B., and Hoffmann, F. M. (2005). Selective inhibition of TGF-β responsive genes by Smad-interacting peptide aptamers from FoxH1, Lef1 and CBP. Oncogene *24*, 3864–3874.

DaCosta Byfield, S., Major, C., Laping, N. J., and Roberts, A. B. (2004). SB-505124 is a selective inhibitor of transforming growth factor-beta type I receptors ALK4, ALK5, and ALK7. Mol. Pharmacol. *65*, 744–752.

Daniels, C. E., Wilkes, M. C., Edens, M., Kottom, T. J., Murphy, S. J., Limper, A. H., and Leof, E. B. (2004). Imatinib mesylate inhibits the profibrogenic activity of TGF-beta and prevents bleomycin-mediated lung fibrosis. J. Clin. Invest. *114*, 1308–1316.

Derynck, R., Akhurst, R. J., and Balmain, A. (2001). TGF-beta signaling in tumor suppression and cancer progression. Nat. Genet. *29*, 117–129.

Derynck, R., and Zhang, Y. E. (2003). Smad-dependent and Smad-independent pathways in TGF-beta family signalling. Nature *425*, 577–584.

Di Guglielmo, G. M., Le Roy, C., Goodfellow, A. F., and Wrana, J. L. (2003). Distinct endocytic pathways regulate TGF-beta receptor signalling and turnover. Nat. Cell Biol. *5*, 410–421.

Dong, C., Li, Z., Alvarez, R., Jr., Feng, X. H., and Goldschmidt-Clermont, P. J. (2000). Microtubule binding to Smads may regulate TGF beta activity. Mol. Cell. *5*, 27–34.

Dumont, N., and Arteaga, C. L. (2003). Targeting the TGFβ signaling network in human neoplasia. Cancer Cell *3*, 531–536.

Ebisawa, T., Fukuchi, M., Murakami, G., Chiba, T., Tanaka, K., Imamura, T., and Miyazono, K. (2001). Smurf1 interacts with transforming growth factor-beta type I receptor through Smad7 and induces receptor degradation. J. Biol. Chem. *276*, 12477–12480.

Edlund, S., Bu, S., Schuster, N., Aspenstrom, P., Heuchel, R., Heldin, N. E., ten Dijke, P., Heldin, C. H., and Landstrom, M. (2003). Transforming growth factor-beta1 (TGF-beta)-induced apoptosis of prostate cancer cells involves Smad7-dependent activation of p38 by TGF-beta-activated kinase 1 and mitogen-activated protein kinase kinase 3. Mol. Biol. Cell *14*, 529–544.

Edlund, S., Landstrom, M., Heldin, C. H., and Aspenstrom, P. (2004). Smad7 is required for TGF-beta-induced activation of the small GTPase Cdc42. J. Cell Sci. *117*, 1835–1847.

Edlund, S., Lee, S. Y., Grimsby, S., Zhang, S., Aspenstrom, P., Heldin, C. H., and Landstrom, M. (2005). Interaction between Smad7 and beta-catenin: importance for transforming growth factor beta-induced apoptosis. Mol. Cell. Biol. *25*, 1475–1488.

Fabbrizio, E., Le Cam, L., Polanowska, J., Kaczorek, M., Lamb, N., Brent, R., and Sardet, C. (1999). Inhibition of mammalian cell proliferation by genetically selected peptide aptamers that functionally antagonize E2F activity. Oncogene *18*, 4357–4363.

Fakhrai, H., Dorigo, O., Shawler, D. L., Lin, H., Mercola, D., Black, K. L., Royston, I., and Sobol, R. E. (1996). Eradication of established intracranial rat gliomas by transforming growth factor beta antisense gene therapy. Proc. Natl. Acad. Sci. USA *93*, 2909–2914.

Feng, X. H., and Derynck, R. (2005). Specificity and versatility in tgf-beta signaling through Smads. Annu. Rev. Cell Dev. Biol. *21*, 659–693.

Flanders, K. C. (2004). Smad3 as a mediator of the fibrotic response. Int. J. Exp. Pathol. *85*, 47–64.

Gorelik, L., and Flavell, R. A. (2001). Immune-mediated eradication of tumors through the blockade of transforming growth factor-beta signaling in T cells. Nat. Med. *7*, 1118–1122.

Gotzmann, J., Mikula, M., Eger, A., Schulte-Hermann, R., Foisner, R., Beug, H., and Mikulits, W. (2004). Molecular aspects of epithelial cell plasticity: implications for local tumor invasion and metastasis. Mutat. Res. *566*, 9–20.

Grygielko, E. T., Martin, W. M., Tweed, C., Thornton, P., Harling, J., Brooks, D. P., and Laping, N. J. (2005). Inhibition of gene markers of fibrosis with a novel inhibitor of transforming growth factor-beta type I receptor kinase in puromycin-induced nephritis. J. Pharmacol. Exp. Ther. *313*, 943–951.

Hjelmeland, M. D., Hjelmeland, A. B., Sathornsumetee, S., Reese, E. D., Herbstreith, M. H., Laping, N. J., Friedman, H. S., Bigner, D. D., Wang, X. F., and Rich, J. N. (2004). SB-431542, a small molecule transforming growth factor-beta-receptor antagonist, inhibits human glioma cell line proliferation and motility. Mol. Cancer Ther. *3*, 737–745.

Hoodless, P. A., Tsukazaki, T., Nishimatsu, S.-i., Attisano, L., Wrana, J. L., and Thomsen, G. H. (1999). Dominant-negative Smad2 mutants inhibit activin/Vg1 signaling and disrupt axis formation in *Xenopus*. Dev. Biol. *207*, 364–379.

Huang, T. T., Wuerzberger-Davis, S. M., Seufzer, B. J., Shumway, S. D., Kurama, T., Boothman, D. A., and Miyamoto, S. (2000). NF-kappaB activation by camptothecin. A linkage between nuclear DNA damage and cytoplasmic signaling events. J. Biol. Chem. *275*, 9501–9509.

Huber, M. A., Azoitei, N., Baumann, B., Grunert, S., Sommer, A., Pehamberger, H., Kraut, N., Beug, H., and Wirth, T. (2004). NF-kappaB is essential for epithelial-mesenchymal transition and metastasis in a model of breast cancer progression. J. Clin. Invest *114*, 569–581.

Inman, G. J., Nicolas, F. J., Callahan, J. F., Harling, J. D., Gaster, L. M., Reith, A. D., Laping, N. J., and Hill, C. S. (2002a). SB-431542 is a potent and specific inhibitor of transforming growth factor-beta superfamily type I activin receptor-like kinase (ALK) receptors ALK4, ALK5, and ALK7. Mol. Pharmacol. *62*, 65–74.

Inman, G. J., Nicolas, F. J., and Hill, C. S. (2002b). Nucleocytoplasmic shuttling of Smads 2, 3, and 4 permits sensing of TGF-beta receptor activity. Mol. Cell *10*, 283–294.

Itoh, F., Divecha, N., Brocks, L., Oomen, L., Janssen, H., Calafat, J., Itoh, S., and ten Dijke, P. (2002). The FYVE domain in Smad anchor for receptor activation (SARA) is sufficient for localization of SARA in early endosomes and regulates TGF-beta/Smad signalling. Genes Cells *7*, 321–331.

Itoh, S., Thorikay, M., Kowanetz, M., Moustakas, A., Itoh, F., Heldin, C. H., and ten Dijke, P. (2003). Elucidation of Smad requirement in transforming growth factor-beta type I receptor-induced responses. J. Biol. Chem. *278*, 3751–3761.

Kasuga, H., Ito, Y., Sakamoto, S., Kawachi, H., Shimizu, F., Yuzawa, Y., and Matsuo, S. (2001). Effects of anti-TGF-beta type II receptor antibody on experimental glomerulonephritis. Kidney Int. *60*, 1745–1755.

Kavsak, P., Rasmussen, R. K., Causing, C. G., Bonni, S., Zhu, H., Thomsen, G. H., and Wrana, J. L. (2000). Smad7 binds to Smurf2 to form an E3 ubiquitin ligase that targets the TGF beta receptor for degradation. Mol. Cell *6*, 1365–1375.

Kennedy, G., and Sugden, B. (2003). EBNA-1, a bifunctional transcriptional activator. Mol. Cell. Biol. *23*, 6901–6908.

Kolb, M., Margetts, P. J., Sime, P. J., and Gauldie, J. (2001). Proteoglycans decorin and biglycan differentially modulate TGF-beta-mediated fibrotic responses in the lung. Am. J. Physiol. Lung Cell Mol. Physiol. *280*, L1327–L1334.

Komesli, S., Vivien, D., and Dutartre, P. (1998). Chimeric extracellular domain type II transforming growth factor (TGF)-beta receptor fused to the Fc region of human immunoglobulin as a TGF-beta antagonist. Eur. J. Biochem. *254*, 505–513.

Lallemand, F., Mazars, A., Prunier, C., Bertrand, F., Kornprost, M., Gallea, S., Roman-Roman, S., Cherqui, G., and Atfi, A. (2001). Smad7 inhibits the survival nuclear factor kappaB and potentiates apoptosis in epithelial cells. Oncogene *20*, 879–884.

Landstrom, M., Heldin, N. E., Bu, S., Hermansson, A., Itoh, S., ten Dijke, P., and Heldin, C. H. (2000). Smad7 mediates apoptosis induced by transforming growth factor beta in prostatic carcinoma cells. Curr. Biol. *10*, 535–538.

Laping, N. J. *et al.* (2002). Inhibition of transforming growth factor (TGF)-beta1-induced extracellular matrix with a novel inhibitor of the TGF-beta type I receptor kinase activity: SB-431542. Mol. Pharmacol. *62*, 58–64.

Leask, A., and Abraham, D. J. (2004). TGF-beta signaling and the fibrotic response. FASEB J. *18*, 816–827.

Li, W. *et al.* (2003a). Squamous cell carcinoma and mammary abscess formation through squamous metaplasia in Smad4/Dpc4 conditional knockout mice. Development *130*, 6143–6153.

Li, Y., Yang, J., Dai, C., Wu, C., and Liu, Y. (2003b). Role for integrin-linked kinase in mediating tubular epithelial to mesenchymal transition and renal interstitial fibrogenesis. J. Clin. Invest *112*, 503–516.

Macias-Silva, M., Abdollah, S., Hoodless, P. A., Pirone, R., Attisano, L., and Wrana, J. L. (1996). MADR2 is a substrate of the TGFbeta receptor and its phosphorylation is required for nuclear accumulation and signaling. Cell *87*, 1215–1224.

Massague, J., Seoane, J., and Wotton, D. (2005). Smad transcription factors. Genes Dev. *19*, 2783–2810.

Mead, A. L., Wong, T. T., Cordeiro, M. F., Anderson, I. K., and Khaw, P. T. (2003). Evaluation of anti-TGF-beta2 antibody as a new postoperative anti-scarring agent in glaucoma surgery. Invest. Ophthalmol. Vis. Sci. *44*, 3394–3401.

Mochizuki, T., Miyazaki, H., Hara, T., Furuya, T., Imamura, T., Watabe, T., and Miyazono, K. (2004). Roles for the MH2 domain of Smad7 in the specific inhibition of transforming growth factor-beta superfamily signaling. J. Biol. Chem. *279*, 31568–31574.

Mori, Y., Ishida, W., Bhattacharyya, S., Li, Y., Platanias, L. C., and Varga, J. (2004). Selective inhibition of activin receptor-like kinase 5 signaling blocks profibrotic transforming growth factor beta responses in skin fibroblasts. Arthritis Rheum. *50*, 4008–4021.

Murakami, G., Watabe, T., Takaoka, K., Miyazono, K., and Imamura, T. (2003). Cooperative inhibition of bone morphogenetic protein signaling by Smurf1 and inhibitory Smads. Mol. Biol. Cell *14*, 2809–2817.

Nagel-Wolfrum, K., Buerger, C., Wittig, I., Butz, K., Hoppe-Seyler, F., and Groner, B. (2004). The interaction of specific peptide aptamers with the DNA binding domain and the dimerization domain of the transcription factor Stat3 inhibits transactivation and induces apoptosis in tumor cells. Mol. Cancer Res. *2*, 170–182.

Nakao, A., Afrakhte, M., Moren, A., Nakayama, T., Christian, J. L., Heuchel, R., Itoh, S., Kawabata, M., Heldin, N. E., Heldin, C. H., and ten Dijke, P. (1997). Identification of Smad7, a TGFbeta-inducible antagonist of TGF-beta signalling. Nature *389*, 631–635.

Nicolas, F. J., and Hill, C. S. (2003). Attenuation of the TGF-beta-Smad signaling pathway in pancreatic tumor cells confers resistance to TGF-beta-induced growth arrest. Oncogene *22*, 3698–3711.

Oft, M., Akhurst, R. J., and Balmain, A. (2002). Metastasis is driven by sequential elevation of H-ras and Smad2 levels. Nat. Cell Biol. *4*, 487–494.

Oft, M., Heider, K. H., and Beug, H. (1998). TGFbeta signaling is necessary for carcinoma cell invasiveness and metastasis. Curr. Biol. *8*, 1243–1252.

Oft, M., Peli, J., Rudaz, C., Schwarz, H., Beug, H., and Reichmann, E. (1996). TGF-beta1 and Ha-Ras collaborate in modulating the phenotypic plasticity and invasiveness of epithelial tumor cells. Genes Dev. *10*, 2462–2477.

Ory, D. S., Neugeboren, B. A., and Mulligan, R. C. (1996). A stable human-derived packaging cell line for production of high titer retrovirus/vesicular stomatitis virus G pseudotypes. Proc. Natl. Acad. Sci. USA *93*, 11400–11406.

Piek, E., Moustakas, A., Kurisaki, A., Heldin, C., and ten Dijke, P. (1999). TGF-(beta) type I receptor/ALK-5 and Smad proteins mediate epithelial to mesenchymal transdifferentiation in NMuMG breast epithelial cells. J. Cell Sci. *112*, 4557–4568.

Qin, B. Y., Lam, S. S., Correia, J. J., and Lin, K. (2002). Smad3 allostery links TGF-beta receptor kinase activation to transcriptional control. Genes Dev. *16*, 1950–1963.

Saika, S. *et al.* (2004). Smad3 signaling is required for epithelial-mesenchymal transition of lens epithelium after injury. Am. J. Pathol. *164*, 651–663.

Santiago, B., Gutierrez-Canas, I., Dotor, J., Palao, G., Lasarte, J. J., Ruiz, J., Prieto, J., Borras-Cuesta, F., and Pablos, J. L. (2005). Topical application of a peptide inhibitor of transforming growth factor-beta1 ameliorates bleomycin-induced skin fibrosis. J. Invest. Dermatol. *125*, 450–455.

Sasaki, A., Masuda, Y., Ohta, Y., Ikeda, K., and Watanabe, K. (2001). Filamin associates with Smads and regulates transforming growth factor-beta signaling. J. Biol. Chem. *276*, 17871–17877.

Sato, M., Muragaki, Y., Saika, S., Roberts, A. B., and Ooshima, A. (2003). Targeted disruption of TGF-beta1/Smad3 signaling protects against renal tubulointerstitial fibrosis induced by unilateral ureteral obstruction. J. Clin. Invest. *112*, 1486–1494.

Savagner, P. (2001). Leaving the neighborhood: molecular mechanisms involved during epithelial-mesenchymal transition. Bioessays *23*, 912–923.

Schmierer, B., and Hill, C. S. (2005). Kinetic analysis of Smad nucleocytoplasmic shuttling reveals a mechanism for transforming growth factor beta-dependent nuclear accumulation of Smads. Mol. Cell. Biol. *25*, 9845–9858.

Shi, W., Sun, C., He, B., Xiong, W., Shi, X., Yao, D., and Cao, X. (2004). GADD34-PP1c recruited by Smad7 dephosphorylates TGFbeta type I receptor. J. Cell Biol. *164*, 291–300.

Shi, Y., and Massague, J. (2003). Mechanisms of TGF-beta signaling from cell membrane to the nucleus. Cell *113*, 685–700.

Shook, D., and Keller, R. (2003). Mechanisms, mechanics and function of epithelial-mesenchymal transitions in early development. Mech. Dev. *120*, 1351–1383.

Siegel, P. M., and Massague, J. (2003). Cytostatic and apoptotic actions of TGF-beta in homeostasis and cancer. Nat. Rev. Cancer *3*, 807–821.

Singh, J., Ling, L. E., Sawyer, J. S., Lee, W. C., Zhang, F., and Yingling, J. M. (2004). Transforming the TGFbeta pathway: convergence of distinct lead generation strategies on a novel kinase pharmacophore for TbetaRI (ALK5). Curr. Opin. Drug Discov. Dev. *7*, 437–445.

Skerra, A. (2000). Engineered protein scaffolds for molecular recognition. J. Mol. Recognit. *13*, 167–187.

Souchelnytskyi, S., Nakayama, T., Nakao, A., Moren, A., Heldin, C. H., Christian, J. L., and ten Dijke, P. (1998). Physical and functional interaction of murine and *Xenopus* Smad7 with bone morphogenetic protein receptors and transforming growth factor-beta receptors. J. Biol. Chem. *273*, 25364–25370.

ten Dijke, P., Goumans, M. J., Itoh, F., and Itoh, S. (2002). Regulation of cell proliferation by Smad proteins. J. Cell. Physiol. *191*, 1–16.

ten Dijke, P., and Hill, C. S. (2004). New insights into TGF-beta-Smad signalling. Trends Biochem. Sci. *29*, 265–273.

Thiery, J. P. (2002). Epithelial-mesenchymal transitions in tumour progression. Nat. Rev. Cancer *2*, 442–454.

Thiery, J. P. (2003). Epithelial-mesenchymal transitions in development and pathologies. Curr. Opin. Cell Biol. *15*, 740–746.

Tsukazaki, T., Chiang, T. A., Davison, A. F., Attisano, L., and Wrana, J. L. (1998). SARA, a FYVE domain protein that recruits Smad2 to the TGFbeta receptor. Cell *95*, 779–791.

Undevia, N. S., Dorscheid, D. R., Marroquin, B. A., Gugliotta, W. L., Tse, R., and White, S. R. (2004). Smad and p38-MAPK signaling mediates apoptotic effects of transforming growth factor-beta1 in human airway epithelial cells. Am. J. Physiol. Lung Cell Mol. Physiol. *287*, L515–L524.

Valcourt, U., Kowanetz, M., Niimi, H., Heldin, C. H., and Moustakas, A. (2005). TGF-beta and the Smad signaling pathway support transcriptomic reprogramming during epithelial-mesenchymal cell transition. Mol. Biol. Cell *16*, 1987–2002.

Warner, D. R., Pisano, M. M., and Greene, R. M. (2003). Nuclear convergence of the TGFbeta and cAMP signal transduction pathways in murine embryonic palate mesenchymal cells. Cell Signal. *15*, 235–242.

Wu, G., Chen, Y. G., Ozdamar, B., Gyuricza, C. A., Chong, P. A., Wrana, J. L., Massague, J., and Shi, Y. (2000). Structural basis of Smad2 recognition by the Smad anchor for receptor activation. Science *287*, 92–97.

Xie, L., Law, B. K., Chytil, A. M., Brown, K. A., Aakre, M. E., and Moses, H. L. (2004). Activation of the Erk pathway is required for TGF-beta1-induced EMT in vitro. Neoplasia *6*, 603–610.

Xu, L., Alarcon, C., Col, S., and Massague, J. (2003). Distinct domain utilization by Smad3 and Smad4 for nucleoporin interaction and nuclear import. J. Biol. Chem. *278*, 42569–42577.

Xu, L., Chen, Y. G., and Massague, J. (2000). The nuclear import function of Smad2 is masked by SARA and unmasked by TGFbeta-dependent phosphorylation. Nat. Cell Biol. *2*, 559–562.

Xu, L., Kang, Y., Col, S., and Massague, J. (2002). Smad2 nucleocytoplasmic shuttling by nucleoporins CAN/Nup214 and Nup153 feeds TGFbeta signaling complexes in the cytoplasm and nucleus. Mol. Cell *10*, 271–282.

Xue, C., Plieth, D., Venkov, C., Xu, C., and Neilson, E. G. (2003). The gatekeeper effect of epithelial-mesenchymal transition regulates the frequency of breast cancer metastasis. Cancer Res. *63*, 3386–3394.

Yingling, J. M., Blanchard, K. L., and Sawyer, J. S. (2004). Development of TGF-beta signalling inhibitors for cancer therapy. Nat. Rev. Drug Discov. *3*, 1011–1022.

Yu, L., Hebert, M. C., and Zhang, Y. E. (2002). TGF-beta receptor-activated p38 MAP kinase mediates Smad-independent TGF-beta responses. EMBO J. *21*, 3749–3759.

Zavadil, J., Cermak, L., Soto-Nieves, N., and Bottinger, E. P. (2004). Integration of TGF-beta/Smad and Jagged1/Notch signalling in epithelial-to-mesenchymal transition. EMBO J. *23*, 1155–1165.

Zeisberg, M., and Kalluri, R. (2004). The role of epithelial-to-mesenchymal transition in renal fibrosis. J. Mol. Med. *82*, 175–181.

Ziyadeh, F. N., Hoffman, B. B., Han, D. C., Iglesias-De La Cruz, M. C., Hong, S. W., Isono, M., Chen, S., McGowan, T. A., and Sharma, K. (2000). Long-term prevention of renal insufficiency, excess matrix gene expression, and glomerular mesangial matrix expansion by treatment with monoclonal antitransforming growth factor-beta antibody in db/db diabetic mice. Proc. Natl. Acad. Sci. USA *97*, 8015–8020.